Results in Physics 19 (2020) 103527

Contents lists available at ScienceDirect

Results in Physics

journal homepage: www.elsevier.com/locate/rinp

2D slab models of TiO_2 nanotubes for simulation of water adsorption: Validation over a diameter range

Oleg Lisovski [a,b,*], Sergei Piskunov [a], Dmitry Bocharov [a,c], Stephane Kenmoe [b]

[a] Institute of Solid State Physics, University of Latvia, Riga LV-1063, Latvia
[b] Department of Theoretical Chemistry, University of Duisburg-Essen, Essen D-45141, Germany
[c] Transport and Telecommunication Institute, Riga LV-1019, Latvia

ARTICLE INFO

Keywords:
Nanotubes
TiO_2
Water adsorption
Slab model
DFT
Water splitting

ABSTRACT

Currently a lot of attention is paid to 1D nanomaterials due to their advantages in comparison to bulk materials. They offer broad possibilities of application, including photocatalytic water splitting. Simulations of water adsorption on such materials with computationally costly theoretical methods, such as *ab initio* molecular dynamics, are needed for improvement of such photocatalysts' efficiency. Still, it is very problematic to treat a real-size nanotube at available computational power. The existing nanotube surface approximations are not accurate and universal enough.

We have already proposed methods for 2D model construction out of TiO_2 nanotubes of (101) and (001) configuration at the moderately expensive DFT level. The idea behind was to provide a partial description of nanotubular strain by applying lattice constants from nanotubes to slab models, and preserving geometry motifs. We use water adsorption energy, valence band maximum and conduction band minimum positions, as well as DOS shape as criteria for model validation.

Our previous work was limited only to specific variants of nanotubes and water adsorption. In this work we establish these novel approaches along a wide nanotube diameter range, in particular for water adsorption studies. We demonstrate that the 2D models do not impose critical compromises in terms of accuracy, and therefore allow calculations of much larger nanotubes than common approaches do.

Introduction

Titanium dioxide has been used for decades as a promising photocatalyst for water splitting. This stems from its numerous beneficial properties such as abundance, low price, non-toxicity, good charge separation and migration. Also, the suitable alignment of conduction band minimum (CBM) with respect to water redox potential has made it a potential candidate for hydrogen evolution in the photocatalytic water splitting reaction. However, the lower position of its valence band maximum (VBM) leads to a wide band gap (3.2 eV), much larger than the threshold for visible-light-driven water splitting [1].

One-dimensional (1D) structures, such as nanorods, nanowires and nanotubes, are considered as prospective materials in many fields, including photocatalytic water splitting. Compared to their bulk and two-dimensional counterparts, 1D nanostructures exhibit unique properties. Because of their thin walls, nanotubes particularly show advantageous properties such as shorter charge travel distances and, consequently, better charge separation, compared to filled 1D materials, such as rods and wires [2].

In spite of all these advantages, nanostructuring by forming TiO_2 nanotubes yields a larger band gap due to size-induced blue shift effect. This has motivated previous studies in our group [3] which provided recipes for keeping TiO_2 nanotubes band gap in the required range for photocatalytic water splitting. The effect of metal and anion doping was investigated by doping the NTs with different foreign atoms (Fe, C, N, S), and it was shown that NTs with S + N co-dopants exhibit suitable redox properties for water splitting reaction. Namely, the VBM and CBM sit accordingly with respect to redox levels for hydrogen and oxygen evolution reactions.

Despite the fact that NTs of various chemical composition, including TiO_2, are successfully synthesized and studied experimentally [2], theoretical investigations on NTs *in operando* are scarce. This is due to

* Corresponding author.
E-mail addresses: Olegs.Lisovskis@cfi.lu.lv (O. Lisovski), piskunov@cfi.lu.lv (S. Piskunov), bocharov@latnet.lv (D. Bocharov), stephane.kenmoe@uni-due.de (S. Kenmoe).

https://doi.org/10.1016/j.rinp.2020.103527
Received 16 June 2020; Received in revised form 11 October 2020; Accepted 18 October 2020
Available online 22 October 2020
2211-3797/© 2020 The Authors. Published by Elsevier B.V. This is an open access article under the CC BY-NC-ND license (http://creativecommons.org/licenses/by-nc-nd/4.0/).

the fact that calculations of real-size 1D nanostructures are too expensive. For example, experimentally accessible TiO_2 NTs have diameters of 10 nm and higher with thousands of atoms. Exploiting the rototranslational symmetry of 1D structures (as implemented in e.g. CRYSTAL [4] code) to reduce the computational costs does not provide a solution, for example in cases of contact with adsorbates in disordered phases like water. In the meanwhile, simulations of NTs with water adsorbed on inner or outer surface (or both simultaneously) are crucial for atomistic-level understanding of photocatalytic water splitting processes.

In literature there are descriptions of alternative approaches to model mechanical [5,6] and electronic [7,8] properties of NTs via a non-periodic cluster describing a fragment of a nanotube. This approach provides reduced size effect for the adsorption energy. However, the lack of periodicity is a limiting factor which yields unphysical boundary effects and therefore a poorer description of the electronic structure. Another, the so-called zone-folding approach also exists [9–11], and is used for calculation of thermodynamic properties of NTs, for example heat capacity and internal energy. Within this approach properties of a NT are defined via an approximation from the slab they are rolled-up from. This method has the advantage of periodicity exploitation, but on the other hand misses taking NT curvature into account.

The problem of accelerating costly calculations, such as *ab initio* MD, can also be approached from another side. For example, new software is developed from scratch with the aim to use massive parallelism of graphics processing units [12]. Other developers employ the machine learning methods [13] or neural network approaches [14] in order to facilitate calculations. Accelerating *ab initio* molecular dynamics simulations by linear prediction methods for molecular systems is reported in [15].

Our group has done its contribution to facilitating costly simulations by developing a model-construction method that is free from the two problems mentioned in alternative model-building approach-related paragraph, namely, lack of periodicity and neglectance of NT curvature. The approach consists in using 2D periodic slabs to model nanotubular surfaces. The mathematical formalism behind this approach was explained in details in [16] and it was later on successfully used to perform molecular dynamics simulations of water adsorption on anatase (36,0) TiO_2 (0 0 1) NTs [17].

Our previous paper [16] focused on developing 2D models for TiO_2 NTs of one specific size for each configuration: 4.2 nm for the thinner (101) NT (0,12) with 6 unique atoms (non-equivalent by symmetry) placed rather aside in the wall, and 4.8 nm for the thicker (001) NT (36,0) with 9 unique atoms placed atop in the wall. One of the models, the FVS model (see details below) performed well for water adsorption on the inner surface of (101) NTs. The other, CFVS model, exhibited good results for water adsorption on the outer surface of (001) NTs. While decent accuracy was found for these large NTs in agreement with the fact that an infinitely large NT converges to a 2D slab, the purpose of this paper, in turn, is to check the range of validity of our approach by performing an extensive and systematic study of selected properties over a broad range of diameters, starting from the smallest NTs where strain effects are pronounced to large NT domain where the 2D NT model's properties are likely to converge to those in the simple slab approximation. The (101) configuration NT range encompasses chirality indices starting from (0,8) to (0,50) and diameters from 2.85 nm to 16.50 nm. The (001) NT range, in turn, includes chirality indices from (8,0) to (50,0) and diameters from 1.9 nm to 6.32 nm, respectively. The primary validation criteria are the single water molecule adsorption energy and the band gap edge positions, with DOS shape being auxiliary.

It may be important to mention that changes in band gap are happening upon water adsorption. As has already been mentioned, more complicated methods and more degrees of freedom are required to study the water adsorption process thoroughly. On the other hand, the purpose of this study is to investigate capacity of the 2D models for reproduction of the properties from the full-size NT models, and not the actual water adsorption process itself, so this aspect will not be discussed in detail in this paper.

Computational details

The 2D models of full-size TiO_2 NTs were prepared using hybrid DFT LCAO method with localized Gaussian-type functions (GTFs) with atom-centered basis sets (BS). The program CRYSTAL [4] was used, with a feature allowing to exploit the rototranslational symmetry, which considerably reduces the computational costs. The choice of the hybrid exchange-correlation functional B3LYP with modified non-local HF exchange contribution (reduced from the default value of 20% to 14%) was motivated explicitly in our earlier publication [3]. The chosen basis sets' configurations were: for Ti - in the form of 411sp-311d with the use of efficient core potential (ECP) implemented by Hay and Wadt [18], for O – the full-electron basis set with configuration of 6s–311sp–1d [19], for H – a TZVP basis set [20]. The main idea was to choose a combination of a basis set and exchange-correlation functional that enables the reproduction of the band edges of the bulk material as closely as possible to the experimental one.

The unit cell of the (101) NTs is thin and the radial distances from the principal axis of the NT to every atom are similar, while the unit cell of the (001) NT is thick and the radial distances for non-equivalent atoms are considerably different (see Fig. 1). The (101) NTs' wall is similar for small, medium and large diameters, while (001) NTs possess trenches at smaller diameter with high strain. The trenches gradually get narrower and then close at ~3.15 nm NT diameter, as atoms become packed more densely on the surface (Fig. 1). The chirality index n of a nanotube is equal to the number of elementary units repeated periodically along circumference of a NT. In Tables 1 and 2 the lattice parameters for NTs of both (101) and (001) configurations, with and without water, for a broad range of chirality indices are shown, and chirality indices with their respective diameters are listed.

In our previous study [16], we have built satisfactory models for the inner layer of the thin-walled (101) nanotube, and by applying additional constraints on atoms, for outer layer adsorption of water on the thicker-walled (001) nanotube. In the first case, the Fixed Volume Slab (FVS) model was used. There, the lattice constants of the two-dimensional slab were determined from the corresponding lattice parameters of the NT along its axis and along its circumference (Fig. 2), and kept fixed during geometry optimization. Inner lattice constants were used for simulation of water adsorption on an inner NT surface, and outer constants – for simulation of water adsorption on an outer surface. There is also a choice to take the lattice constants from a full-size NT with or without water.

In the second case, the Constrained Fixed Volume Slab (CFVS) model, an extension of the FVS model was used, see Fig. 3. Construction of this model starts with stratifying a NT wedge so that relative coordinates in a 2D model stay as close to their respective coordinates in a NT unit cell, see the second image in Fig. 3. Absolute atom coordinates expressed as arch lengths in a unit cell must be divided by either a unit-cell-averaged lattice constant b, or arch length for every of the 9 atoms must be divided by its own layer-unique b constant. Hereafter we will refer to these variants as average-b-based and unique-b-based models. Then the resulting relative coordinates must be multiplied by b lattice constant taken from a full-size NT (either outer or inner constant, the outer is used in the particular study), with water or without, same as in FVS model. The positions of NT atoms in the layer opposite to the water adsorption sites were constrained to allow a better description of the strain induced by the NT curvature.

Previously it was shown that the FVS model was suitable for the (101) NTs' inner surface. In turn, the CFVS model proved reasonably accurate for the outer surface of the (001) NTs. We assign this to the difference in unit cell configuration, for more details see [16].

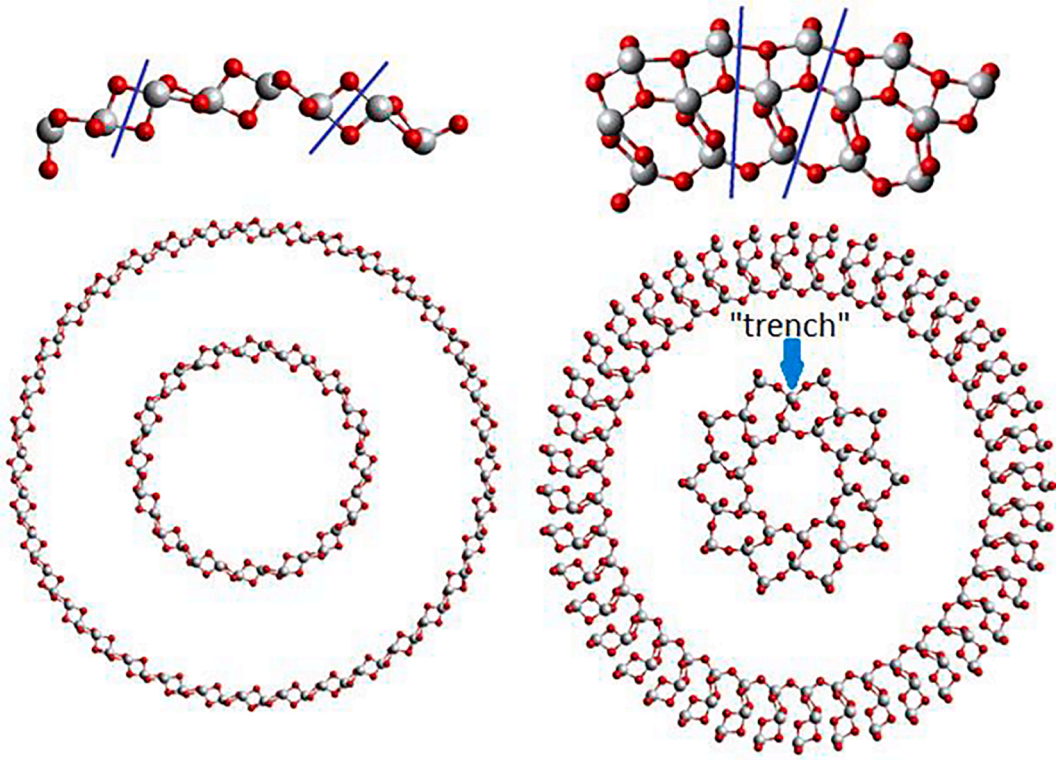

Fig. 1. Comparison of small and large diameter NTs for (101) (0,*n*) (left) and (001) (*n*,0) (right) configurations, respectively. On the (101) configuration the nanotubular wall looks almost identical, while for the (001) NTs there is a prominent difference in structure due to strain and wall thickness. Note that the NTs are not multi-wall; the smaller ones are inserted into the larger ones for space saving. Unit cells of nanotubular walls are shown in the magnified wall fragments with blue lines.

Table 1
Selected parameters of (101) (0,*n*) TiO_2 NTs, calculated without and with water, where *d* stands for inner NT diameter, *a* – lattice parameter parallel to the principal NT axis, b_{inn} – lattice parameter derived from an inner circumference of a NT. "H_2O" in brackets means that the parameter was taken from a NT optimized with water. Note that for the *a* constant there is a slight decreasing trend with some exceptions, but b_{inn} – steadily increases.

(101) NTs (0,*n*)	*d*, Å	*d*, Å (H_2O)	*a*, Å	*a*, Å (H_2O)	Average *a*, Å	b_{inn}, Å	b_{inn}, Å (H_2O)	average b_{inn}, Å	N of atoms in a ringed unit cell
(0,8)	24.16	23.70	3.545	3.665	3.605	9.482	9.301	9.392	96
(0,10)	30.82	30.18	3.537	3.664	3.600	9.676	9.477	9.576	120
(0,12)	37.46	37.46	3.540	3.664	3.602	9.803	9.593	9.698	144
(0,14)	44.12	43.16	3.537	3.663	3.600	9.895	9.679	9.787	168
(0,16)	50.77	49.65	3.535	3.663	3.599	9.963	9.743	9.853	192
(0,18)	57.42	56.15	3.534	3.663	3.598	10.016	9.795	9.905	216
(0,20)	64.06	62.64	3.533	3.663	3.598	10.058	9.834	9.946	240
(0,22)	70.73	69.14	3.531	3.664	3.597	10.095	9.868	9.981	264
(0,24)	77.33	75.65	3.535	3.663	3.599	10.117	9.897	10.007	288
(0,26)	84.03	82.14	3.530	3.664	3.597	10.148	9.920	10.034	312
(0,28)	90.68	88.64	3.529	3.663	3.596	10.169	9.941	10.055	336
(0,30)	97.26	95.15	3.535	3.664	3.599	10.180	9.959	10.070	360
(0,32)	103.91	101.66	3.534	3.664	3.599	10.196	9.975	10.086	384
(0,34)	110.55	108.17	3.534	3.663	3.599	10.210	9.990	10.100	408
(0,36)	117.28	114.66	3.529	3.663	3.596	10.229	10.001	10.115	432
(0,38)	123.85	121.19	3.533	3.664	3.599	10.234	10.014	10.124	456
(0,40)	130.59	127.69	3.529	3.664	3.596	10.251	10.023	10.137	480
(0,50)	163.84	160.24	3.528	3.663	3.595	10.289	10.063	10.176	600

Results

The (101) NTs and 2D FVS model

Fig. 4 shows selected segments of 3 different (101) NTs configurations of small, middle, and large diameter, respectively, and their corresponding FVS models are shown on the right. It can be seen that the structures of the NTs are almost identical for the three different diameters, with the only prominent difference consisting in flattening of the NT wall along with its growth. The water is adsorbed uniformly in all three cases, with the oxygen atom pointing at one of the Ti atoms closer to the inner surface of a NT, and one of the hydrogens pointing to the innermost oxygen on the nanotubular surface.

The larger the NT chirality index *n* is the more the 2D FVS models tend to be similar to the corresponding original NTs, as the curvature effect becomes less pronounced.

Let us consider the first validation criterion of our models, the water adsorption energy, for (101) NTs and their 2D slab models. Since it was shown in our previous work [16] that the FVS model performs better for (101) NTs and water adsorption on their inner surfaces, in the present

Table 2
Parameters of (001) (n,0) TiO_2 NTs, calculated without and with water, where D stands for outer NT diameter, a – lattice parameter parallel to the principal NT axis, b_{out} – lattice parameter derived from an outer NT circumference. "H_2O" in brackets means that the parameter was taken from a NT optimized with water. Note that for the a constant there is a slight increasing trend with some exceptions, but b_{out} – steadily decreases.

(001) NTs (0, n)	D, Å	D, Å (H_2O)	a, Å	a, Å (H_2O)	b_{out}, Å	b_{out}, Å (H_2O)	N of atoms in a ringed unit cell
(8,0)	19.170	19.019	3.390	3.472	7.524	7.465	72
(10,0)	21.983	21.889	3.366	3.399	6.903	6.873	90
(12,0)	24.550	24.152	3.358	3.402	6.424	6.320	108
(14,0)	26.711	26.558	3.362	3.407	5.991	5.957	126
(16,0)	28.673	28.981	3.379	3.413	5.627	5.687	144
(18,0)	30.376	31.345	3.407	3.426	5.299	5.468	162
(20,0)	31.790	31.629	3.444	3.463	4.991	4.966	180
(22,0)	33.469	33.265	3.469	3.497	4.777	4.748	198
(24,0)	35.419	35.310	3.478	3.509	4.634	4.620	216
(26,0)	37.592	37.442	3.486	3.522	4.540	4.522	234
(28,0)	39.706	39.569	3.487	3.527	4.453	4.437	252
(30,0)	41.818	41.700	3.487	3.533	4.377	4.365	270
(32,0)	43.934	43.836	3.486	3.538	4.311	4.301	288
(34,0)	46.052	45.983	3.485	3.542	4.253	4.247	306
(36,0)	48.187	48.137	3.485	3.547	4.203	4.199	324
(38,0)	50.308	50.330	3.485	3.548	4.157	4.159	342
(40,0)	52.510	52.477	3.483	3.556	4.122	4.119	360
(42,0)	54.680	54.650	3.482	3.557	4.088	4.086	378
(44,0)	56.920	56.840	3.481	3.562	4.062	4.056	396
(46,0)	59.141	59.038	3.481	3.565	4.037	4.030	414
(48,0)	61.391	61.232	3.480	3.568	4.016	4.006	432
(50,0)	63.631	63.227	3.480	3.560	3.996	3.971	450

paper we focus on a wide diameter range of such systems. We considered 2D models with lattice constants inherited from full-size (0,n) NTs optimized with and without water. The results for these two cases had roughly equal magnitude of deviation from the reference NT, with different sign. Therefore, it was decided to consider a third variant of the FVS model, with averaged lattice constants.

The water adsorption energy dependence on NTs chirality index is shown in Fig. 5. The cyan horizontal line represents the water adsorption energy on a TiO_2 (101) 6-layer slab, which served as the basis for (101) NT model construction. The blue curve shows the adsorption energy on full-size (101) NTs and is taken as a reference for comparison. The red, green and yellow curves show the adsorption energy for FVS models corresponding to (101) NTs with (0,n) configuration and different chirality index n values. The adsorption energies for FVS model with a and b parameters taken from NT with and without water are shown in yellow and red color, respectively. Finally, water adsorption energy for FVS models with a and b taken as the average of the corresponding lattice constants from NTs optimized with and without water is shown with green.

All curves show similar shape starting from the critical chirality of $n = 20$. With respect to the full-size NT, models with lattice parameters taken from a water-free NT underestimate the binding energy by about 0.7 eV in average, while those built with lattice parameters taken from NT with water overestimate the binding energy by a very similar amount. Interestingly, building models from average values of lattice parameters of water-free and water covered yields more acceptable results. The maximum deviation from the reference NT (green curve) is 15 meV in the range $20 < n < 50$. This observation consolidates the efficiency of this empirical approach that was already proposed in our previous work where it was applied just to a (101) NT (0,12) [16]. Moreover, for large nanotubes domain, this approach yields a fast convergence of models towards 2D surface slabs, faster even than the full-size NT. As it can be seen from Fig. 5, at the vicinity of $n = 50$, the green curve asymptotically converges to the cyan one representing the simple 2D surface slab and crosses the dark blue curve already at $n = 26$.

Below $n = 20$, the curves illustrating the model's variants have a deeper slope compared to the blue one representing the full-size NT reference. Size effects are more pronounced and the deviation of the binding energy from the full-size NT is strongly dependent on the nanotube radius. Models with lattice parameters taken from a water-free NT and those obtained with lattice parameters taken from NT with water show opposite trends. As NT radius increases, the binding energy quickly diverges (already at $n = 10$) from the reference one on the former while a slow convergence is observed on the latter. Both effects are averaged in the third model variant where lattice constants are also averaged.

VB top and CB bottom positions of FVS models and their reference NTs are shown in Fig. 6. The lines' colours denote the same material systems as those in Fig. 5. The reference curve shows a modulated inverse radius dependence. This curve in Fig. 6 starts at 1.0 eV for the CB minimum and slowly decays to approximately 0.65–0.7 eV. Similarly, one can observe a similar slow decay from −3.25 eV to −3.48 eV for the VB maximum.

For $n \geq 20$, the curves for band edge positions for the 2D FVS model variants and the original NTs have similar shape. All the three variants of 2D FVS models overestimate both the VB and CB edges by approximately 0.5 eV in almost the whole range of diameters.

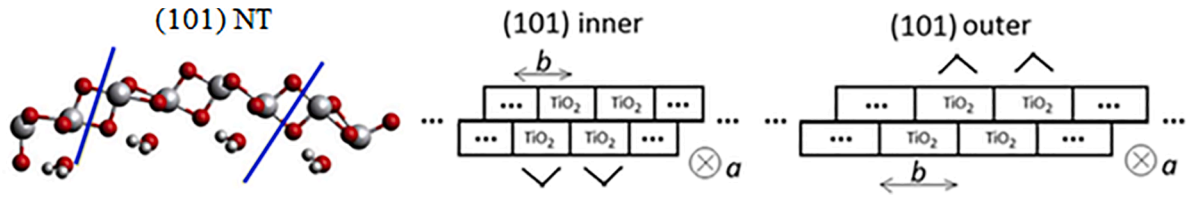

Fig. 2. Illustration of the 2D FVS model principle.

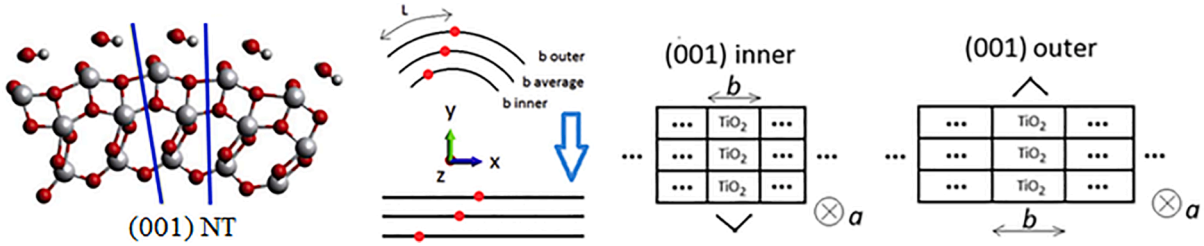

Fig. 3. Illustration of the 2D CFVS model principle.

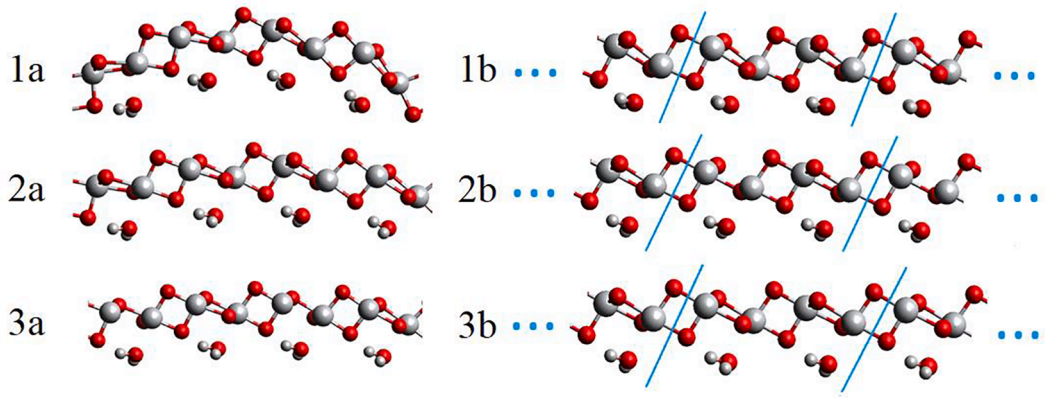

Fig. 4. Fragments of selected (101) NTs with adsorbed water molecules: 1a – NT (0, 10), 2a – NT (0, 22), 3a – NT (0, 40), and their corresponding 2D FVS models with the unit cell delimitated by blue lines.

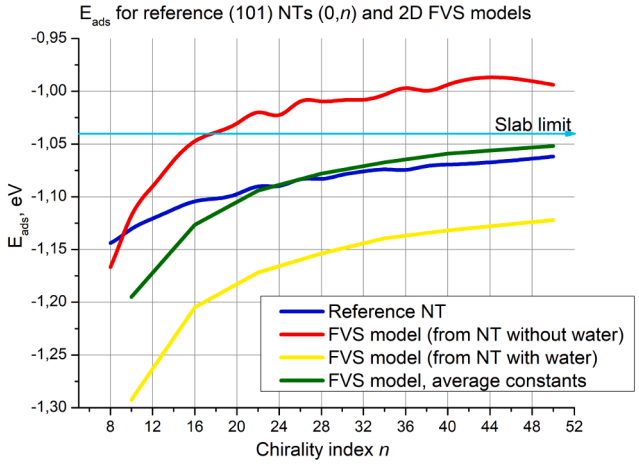

Fig. 5. Water adsorption energy for TiO_2 (101) NTs with different chirality indices (blue curve) used as the reference, and for corresponding 2D FVS models in three variations (red, green and yellow curves). The regular TiO_2 (101) 6-layer slab limit used for (101) NT construction (cyan horizontal line) is also included.

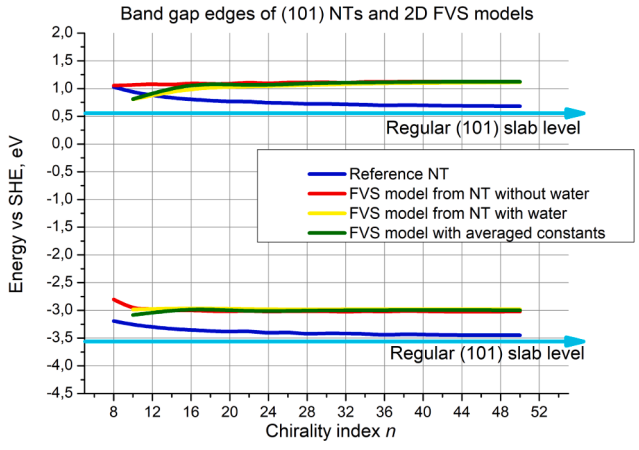

Fig. 6. VB top and CB bottom edge positions for TiO_2 (101) NT with different (0,*n*) chirality indices and for corresponding FVS models.

However, there are differences in the range of the smaller diameters ($n < 20$). The CBM curve for the 2D FVS model with lattice constants from NTs optimized without water starts at the same origin as the reference curve. Then these 2 curves diverge, while the 2D FVS model with lattice constants from NTs optimized with water and the one with the averaged constants originates somewhat below the reference curve and then crosses it.

For all model variants, the VBM curves start above the reference curve. Particularly, the model with lattice constants from NTs optimized without water appears like an almost perfect translation of the reference curve. The two other model variants show curves with opposite slope and weaker steepness.

Despite the general shift of roughly 0.5 eV upward of VB/CB edge positions, the DOS for the full-size (101) NTs and the corresponding 2D FVS models look similar in shape. Due to the limited volume of the article, we include only two pairs of DOS – for the averaged-constant FVS models NT, and for their reference NTs, where one possesses a chirality index *n* smaller than the aforementioned critical value 20, and one – larger, see Figs. 7 and 8.

The (001) TiO_2 nanotube and CFVS model

Fig. 9 shows 3 fragments of full-size (001) NTs of different diameters increasing with order of chirality: (15,0), (22,0), and (28,0). Their corresponding CFVS models are displayed on the right.

The larger the NT gets, the better the corresponding 2D CFVS model mimics its structure. Though the 2D models of the smaller NTs overstretch the inner surface layers due to the constraints applied, they still describe the outer surface layers reasonably.

Fig. 10 shows the dependence of water adsorption energy on TiO_2 (001) NT surface and the corresponding CFVS models for different NT chirality indices. For the reference system corresponding to water adsorption on outer surface of full-size (001) TiO_2 NTs the curve (dark blue) begins at approximately −0.85 eV, then there is a minimum with the lowest point at roughly −1.3 eV. The minimum turns into a slow monotonous growth at chirality index $n = 20$ which lasts until the end of the curve at $n = 50$.

The appearance of a minimum on this curve is due to the differences in geometry for the small and large diameter NTs, as can be seen in Fig. 9. As was indicated above, for the smaller NTs there are “trenches” on the surface which provide more favorable positions for water molecule adsorption, while the trenches vanish starting from the chirality index $n = 20$, thus leading to the beginning of the monotonous growth of the curve.

In general, the 2D CFVS models were able to represent the trend with good agreement to the reference in the range of all diameters: small, medium and large NT. Although there was a general expectation that the 2D CFVS models would fail to represent original NTs in the domain of small diameters, it was not the case, and the 2D model reproduced also the minimum in the left side of the curve, with only a slight shift of the

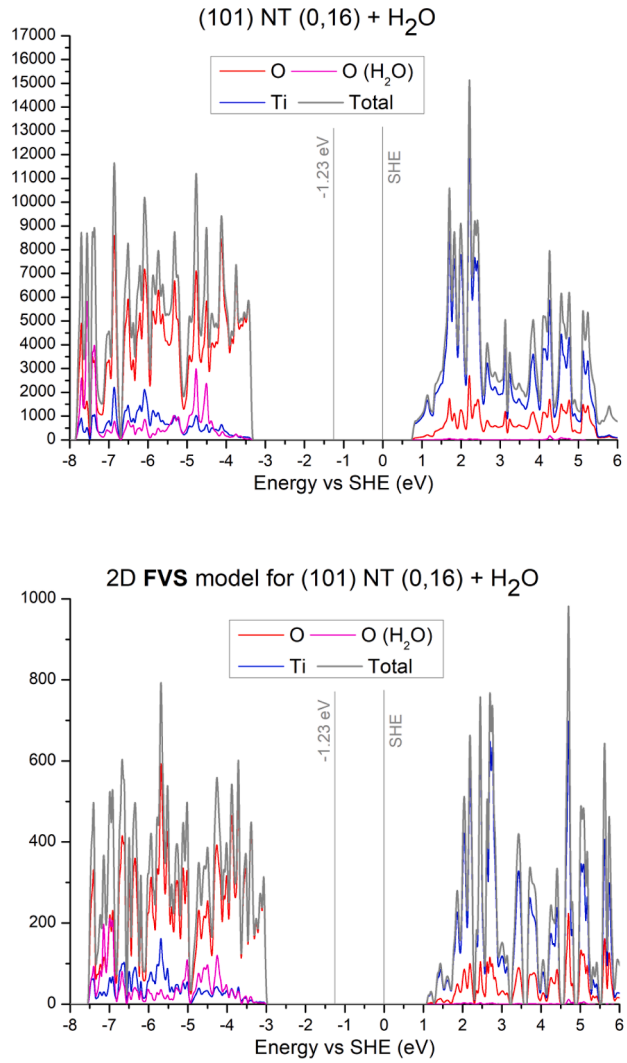

Fig. 7. DOS for (101) NT (0,16) with 1ML water adsorbed, and for the corresponding 2D FVS model with averaged lattice constants and with the same water coverage.

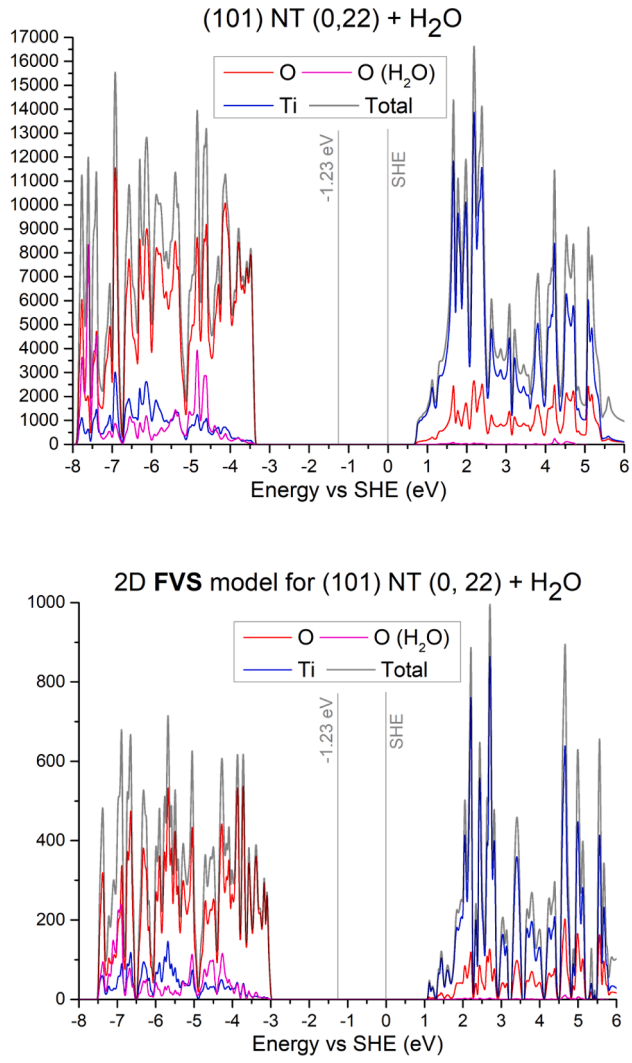

Fig. 8. DOS for (101) NT (0,22) with 1ML water adsorbed, and for the corresponding 2D FVS model with averaged lattice constants and with the same water coverage.

global minimum (chirality index $n = 15$ vs 18) and difference in the minimum depth of ~0.1 eV). This better-than-expected performance must be attributed to the fact that the 2D models of even small NTs reproduce geometry of the outer surface decently.

All of the models perform decently in the range of medium chirality indices ($n = 20$–32), with one exception point for the orange curve. Further on, in the large chirality index range (34–50) the deviation grows to roughly 0.06 eV for 2D model variants which were built by taking lattice parameters of NTs optimized without water. In turn, the models where the lattice parameters were taken from a full-size NT optimized with water yielded prominently better results at these larger diameters.

It is worth mentioning that while for the (101) NTs the reference curve and the curve for the 2D model with averaged lattice constants converge to water adsorption energy slab limit, for the (001) NTs and 2D CFVS models it is not the case, since the nanotubular wall undergoes reconstruction with respect to the slab. The energy cost for this reconstruction makes the water adsorption energy limit somewhat higher than the regular slab adsorption energy.

Before discussing the band gap edges and DOS, it is necessary to mention that specific adjustments are needed when constructing DOS for 2D CFVS models. While for the full-size (001) TiO_2 (NTs) simply all O and Ti atoms have to be taken into consideration when constructing DOS, such an approach applied to CFVS models of the same NTs would result, in particular, in the presence of an unphysical peak within a band gap. One way of correcting this discrepancy, as described in our previous publication [16], is to passivate innermost surface O and one Ti atoms which were kept fixed during geometry optimization with hydrogen atoms, not including the latter into DOS. This approach resulted in a shift of this artificial peak near to the valence band edge. Such adjustments lead to band gap opening. However, the gap width was still underestimated by roughly 0.5 eV, which was attributed to the model's intrinsic imperfections.

In the present study, as the procedure was repeated for a series of (001) TiO_2 NTs, it was noticed that, if these artificial peaks were neglected, the band gap width reproduction would become almost exact, and the discrepancy will remain only in positions of both band edges. So, it was decided not only to passivate 2D CFVS models with hydrogen atoms, but also to exclude the fixed atoms from DOS construction, thereby defining the top of the VB as the highest occupied state attributed to one of the non-fixed atoms.

As is seen in Fig. 11, for the original NT the curves of VBM and CBM positions are almost steady except for a jump at the chirality index $n = 20$, the point where the "trench" on the NT surface gets closed and therefore new bonding situation for the outermost atoms appears. The values of the band gap width are slightly higher for the smallest NTs and

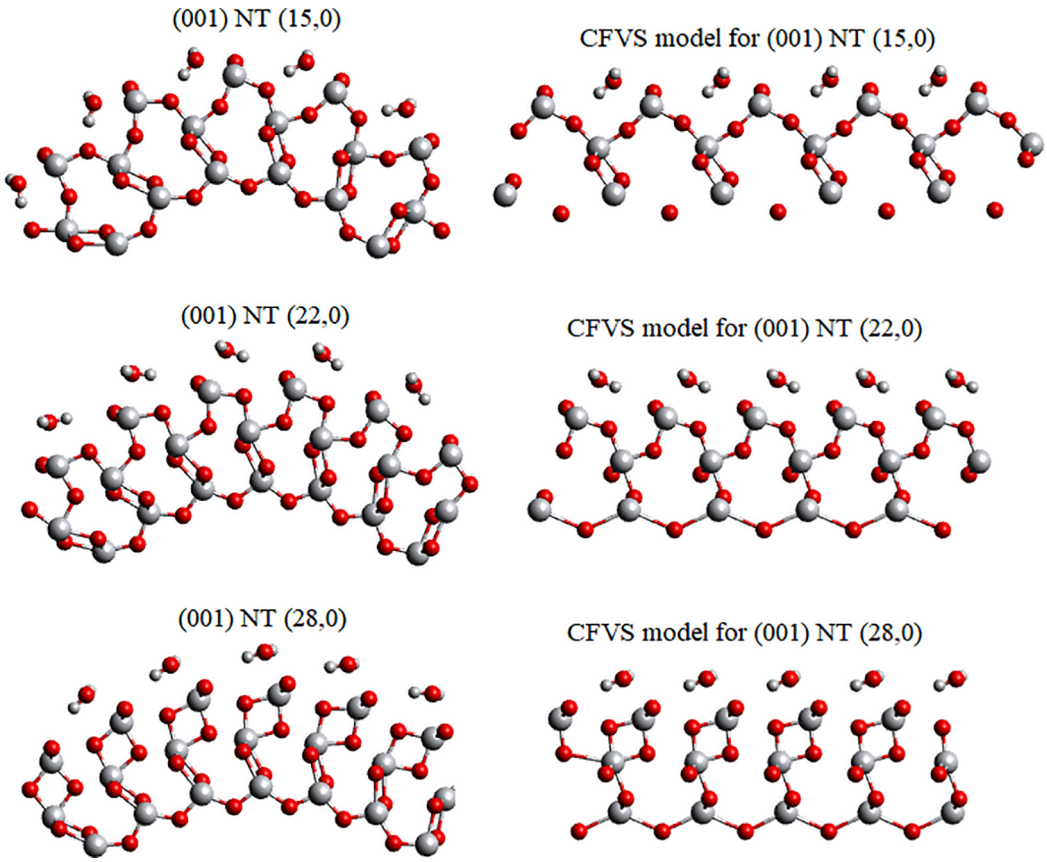

Fig. 9. Optimized structures of several full-size (001) TiO_2 NTs and corresponding CFVS models.

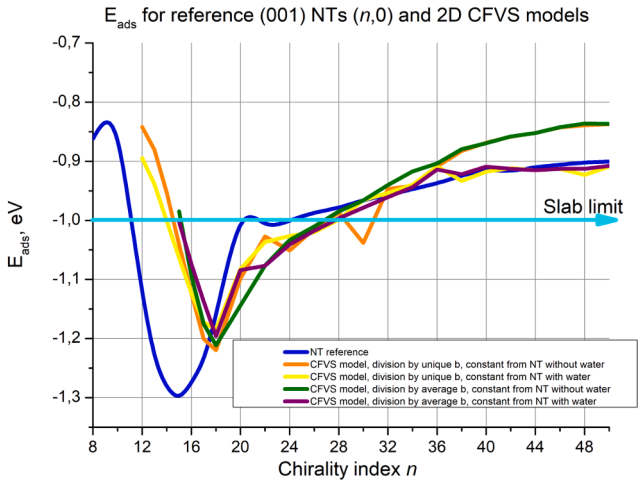

Fig. 10. The water adsorption energy on TiO_2 (001) NTs with different chirality indices (blue curve), used as the reference, together with data on corresponding 2D CFVS models.

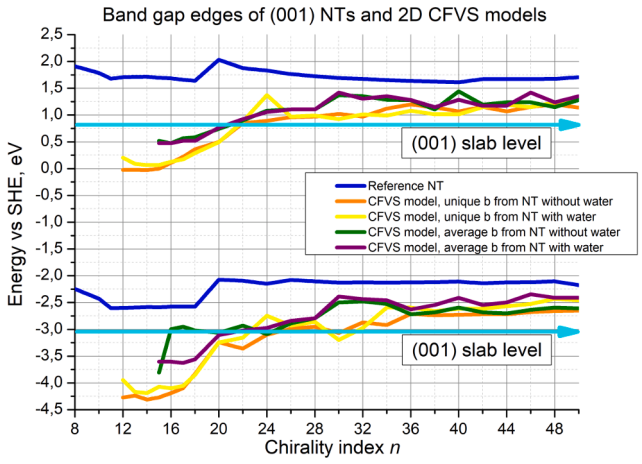

Fig. 11. VB top and CB bottom edge positions for TiO_2 (001) NTs with different (*n*,0) chirality indices and for corresponding CFVS models. The cyan line indicates slab band maxima positions.

are roughly equal to 4.2–4.3 eV, while the band gap is narrower in the larger NT domain with the gap around 3.8 eV. This is in line with size-induced band gap blue shift due to nanostructuring.

In the large and medium diameter domains the 2D CFVS models are able to reproduce the band gap width of the reference NTs rather precisely, with a deviation typically not larger than 0.1–0.2 eV. The positions of the band edges are reproduced less precisely, with both edges for the 2D model being systematically shifted downwards. In the range of the largest NTs (chirality indices 36–50) all models perform rather similarly, with the leading variant being the one built by obtaining relative coordinates via division of arch lengths in a NT unit cell by *b* constant taken as average between all atomic layers, and by further multiplication by outer *b* constant taken from a NT with water. The shift is roughly 0.5 eV for the largest models, which is acceptable. In the medium diameter range (chirality indices 28–36) better performance of models constructed via the averaged *b*, regardless of the presence of water in the NT-origin, is visible. When moving from the largest to the medium-size models, the shift gets larger for the unique-*b*-based 2D models (up to ~1 eV for VBM top and ~0.7 eV for CBM bottom), and roughly the same as for the large NT diameter domain for the average-*b*-

based CFVS models. Below the chirality of 26–28 the deviation becomes prominently larger than 1 eV for all 2D model variants.

We explain the general behaviour of 2D CFVS model graph with the fact that these models partially preserve curvature of the NTs during construction, which is not the case for the FVS model which is built starting from a slab and not a NT. Since the CFVS model contains both slab and NT features, this is the reason why the 2D model curves are located between the NT reference curve and the graph for the simple (001) slab – in the range of medium/large diameters, where performance of the 2D models is better.

Same as in the VBM/CBM graph, there are larger discrepancies in the DOS for the smaller NTs, and the agreement in shape and band edge positions becomes more decent towards the larger NT diameters. Again, due to article volume restriction, we limit ourselves to two pairs of DOS for the unique-*b*-based CFVS models, of a large NT without a trench and a small NT with a trench, with constants taken from NTs without water, and their reference NTs, see Figs. 12 and 13.

Conclusions

In this study we provided a validation for the 2D FVS and CFVS models over a range of nanotubular diameters. We investigated 2D model performance in the range from small NTs with high strain until largest NTs which were accessible by our computational resources.

Water adsorption energies for the (101) NTs were reproduced with high accuracy by the averaged-lattice-constant-based FVS models starting with $n = 20$. For the (001) NTs the CFVS models also yielded a good result on the whole NT size range, reproducing both the general trend and the minimum. The model variants originating from a NT with adsorbed water performed better in the range of larger NTs.

The band edge reproduction was acceptable for FVS models of (101) NTs also starting from $n \sim 20$ with deviations of the 0.5 eV order, while for the CFVS models of (001) NTs the region of the same acceptable deviation of 0.5 eV starts at somewhat larger diameters ($n \sim 30$), with average-*b*-based variants outperforming unique-*b*-based variants. The DOS shapes were satisfactory in general.

To sum up, the 2D FVS model performed well for (101) NTs starting with chirality index $n \sim 20$. The 2D (001) CFVS model performed well for the same NT diameter domain in terms of water adsorption due to good geometry reproduction. Its performance was inferior in terms of electronic structure, with acceptable results starting at NT chirality index $n \sim 30$, but, on the other hand, the CFVS model performed well in

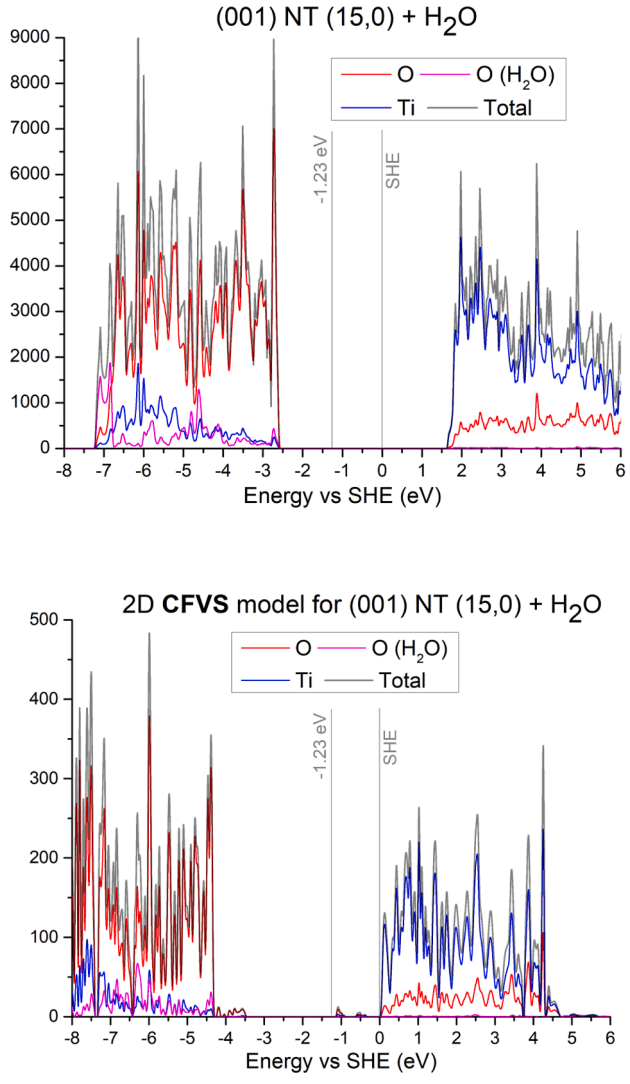

Fig. 12. DOS for (001) NT (15,0) with 1ML water adsorbed, and for the corresponding 2D CFVS model, unique-*b*-based, with constants taken from a NT without water, with the same water coverage. The little peaks within the band gaps are rudiments from the fixed atoms and are ignored when defining VBM and CBM.

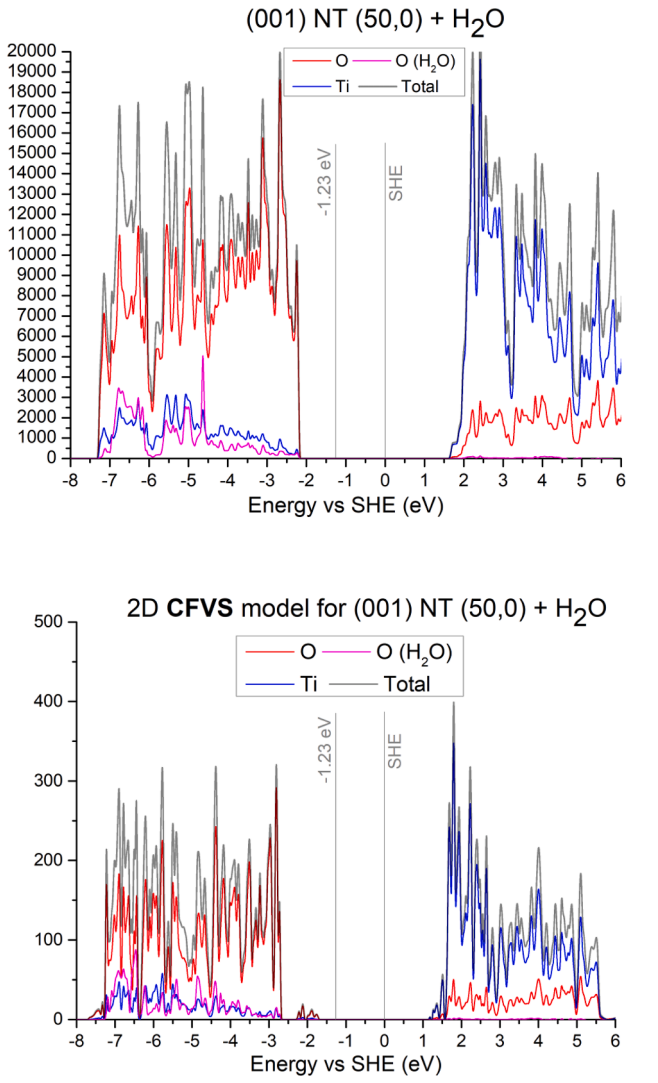

Fig. 13. DOS for (001) NT (50,0) with 1ML water adsorbed, and for the corresponding 2D CFVS model, unique-*b*-based, with constants taken from a NT without water, with the same water coverage. The little peaks within the band gap of the CFVS model are rudiments from the fixed atoms and are ignored when defining VBM and CBM.

terms of water adsorption energy on the whole NT diameter range. These results provide a further confirmation that the approximations to the surfaces of TiO_2 NTs firstly proposed in our initial paper [16] are indeed adequate models working systematically for a wide range of NT diameters except only the small ones, with the highest strain, and can be recommended to be used as a fundament for (101) (0,*n*) and (001) (*n*,0) TiO_2 NT simulation with expensive methods, such as *ab initio* MD. Potentially, these methods can be useful for NTs with similar configuration made of other materials.

CRediT authorship contribution statement

Oleg Lisovski: Conceptualization, Formal analysis, Funding acquisition, Investigation, Methodology, Validation, Visualization, Writing - original draft, Writing - review & editing. **Sergei Piskunov:** Supervision, Writing - review & editing. **Dmitry Bocharov:** Investigation, Visualization, Methodology, Writing - original draft, Writing - review & editing. **Stephane Kenmoe:** Methodology, Writing - original draft, Writing - review & editing.

Declaration of Competing Interest

The authors declare that they have no known competing financial interests or personal relationships that could have appeared to influence the work reported in this paper.

Acknowledgments

Financial support provided by Scientific Research Project for Students and Young Researchers Nr. SJZ/2019/2 realized at the Institute of Solid State Physics, University of Latvia is greatly acknowledged. Institute of Solid State Physics, University of Latvia as the Center of Excellence has received funding from the European Union's Horizon 2020 Framework Programme H2020-WIDESPREAD-01-2016-2017-TeamingPhase2 under Grant Agreement No. 739508, project CAMART^2.

Data availability

The raw/processed data required to reproduce these findings cannot be shared at this time as the data also forms part of an ongoing study.

References

[1] Kudo A, Miseki Y. Heterogeneous photocatalyst materials for water splitting. Chem Soc Rev Jan. 2009;38(1):253–78. https://doi.org/10.1039/b800489g.

[2] Ge M, et al. A review of TiO_2 nanostructured catalysts for sustainable H_2 generation. Int J Hydrogen Energy 2016;42(12):8418–49. https://doi.org/10.1016/j.ijhydene.2016.12.052.

[3] Piskunov S, et al. C-, N-, S-, and Fe-doped TiO_2 and $SrTiO_3$ nanotubes for visible-light-driven photocatalytic water splitting: prediction from first principles. J Phys Chem C 2015;119(32):18686–96. https://doi.org/10.1021/acs.jpcc.5b03691.

[4] Dovesi R, et al., Crystal'17 User's Manual. 2018.

[5] Lu X, Hu Z. Mechanical property evaluation of single-walled carbon nanotubes by finite element modeling. Compos Part B Eng 2012;43(4):1902–13. https://doi.org/10.1016/j.compositesb.2012.02.002.

[6] Mahmoudinezhad E, Ansari R, Basti A, Hemmatnezhad M. An accurate spring-mass finite element model for vibration analysis of single-walled carbon nanotubes. Comput Mater Sci 2014;85:121–6. https://doi.org/10.1016/j.commatsci.2013.11.046.

[7] Sodré JM, Longo E, Taft CA, Martins JBL, dos Santos JD. Electronic structure of GaN nanotubes. Comptes Rendus Chim 2016;20:190–6. https://doi.org/10.1016/j.crci.2016.05.023.

[8] Chesnokov A, et al. *Ab initio* simulations on N and S co-doped titania nanotubes for photocatalytic applications. Phys Scr 2015;90(9):094013. https://doi.org/10.1088/0031-8949/90/9/094013.

[9] Wirtz L, Rubio A, De La Concha R, Loiseau A. *Ab initio* calculations of the lattice dynamics of boron nitride nanotubes. Phys Rev B – Condens Matter Mater Phys 2003;68(4):1–13. https://doi.org/10.1103/PhysRevB.68.045425.

[10] Popov VN, Lambin P. Radius and chirality dependence of the radial breathing mode and the G -band phonon modes of single-walled carbon nanotubes. Phys Rev B – Condens Matter Mater Phys 2006;73(8):1–9. https://doi.org/10.1103/PhysRevB.73.085407.

[11] Porsev VV, Bandura AV, Evarestov RA. Temperature dependence of strain energy and thermodynamic properties of V_2O_5-based single-walled nanotubes: zone-folding approach. J Comput Chem 2016;37(16):1442–50. https://doi.org/10.1002/jcc.24354.

[12] Seritan S, et al. TeraChem: Accelerating electronic structure and *ab initio* molecular dynamics with graphical processing units. J Chem Phys 2020;152(22):224110. https://doi.org/10.1063/5.0007615.

[13] Botu V, Ramprasad R. Adaptive machine learning framework to accelerate *ab initio* molecular dynamics. Int J Quantum Chem 2015;115(16):1074–83. https://doi.org/10.1002/qua.24836.

[14] Wang J, Li C, Shin S, Qi H. Accelerated atomic data production in *Ab Initio* molecular dynamics with recurrent neural network for materials research. J Phys Chem C 2020;124(27):14838–46. https://doi.org/10.1021/acs.jpcc.0c01944.

[15] Herr JD, Steele RP. Accelerating *ab initio* molecular dynamics simulations by linear prediction methods. Chem Phys Lett 2016;661:42–7. https://doi.org/10.1016/j.cplett.2016.08.050.

[16] Lisovski O, Kenmoe S, Piskunov S, Bocharov D, Zhukovskii YF. Validation of a constrained 2D slab model for water adsorption simulation on 1D periodic TiO_2 nanotubes. Comput Condens Matter 2018;15(November 2017):69–78. https://doi.org/10.1016/j.cocom.2017.11.004.

[17] Kenmoe S, Lisovski O, Piskunov S, Bocharov D, Zhukovskii YF, Spohr E. Water adsorption on clean and defective anatase TiO_2 (001) nanotube surfaces: a surface science approach. J Phys Chem B 2018;122(21):5432–40. https://doi.org/10.1021/acs.jpcb.7b11697.

[18] Piskunov S, Heifets E, Eglitis R, Borstel G. Bulk properties and electronic structure of $SrTiO_3$, $BaTiO_3$, $PbTiO_3$ perovskites: an *ab initio* HF/DFT study. Comput Mater Sci 2004;29(2):165–78. https://doi.org/10.1016/j.commatsci.2003.08.036.

[19] Heyd J, Peralta JE, Scuseria GE, Martin RL. Energy band gaps and lattice parameters evaluated with the Heyd-Scuseria-Ernzerhof screened hybrid functional. J Chem Phys 2005;123(17). https://doi.org/10.1063/1.2085170.

[20] Peintinger MF, Oliveira DV, Bredow T. Consistent Gaussian basis sets of triple-zeta valence with polarization quality for solid-state calculations. J Comput Chem 2013;34(6):451–9. https://doi.org/10.1002/jcc.23153.